Epigenetic Immunomodulatory Effect of Eugenol and Astaxanthin on Doxorubicin Cytotoxicity in Hormonal Positive Breast Cancer Cells

Mariam A. Fouad
National Cancer Institute Cairo University
Mohamed M. Sayed-Ahmed
National Cancer Institute Cairo University
Etimad A. Huwait
College of Sciemce,KAU
Hafez F. Hafez
National Cancer Institute Cairo University
Abdel-Mneim M. Osman (moneimosman@hotmail.com)
Fondazione IRCCS Istituto Nazionale dei Tumori

Research article

Keywords: Eugenol, Astaxanthin, Doxorubicin, Breast Cancer Cells

Posted Date: July 14th, 2020

DOI: https://doi.org/10.21203/rs.3.rs-39744/v1

Version of Record: A version of this preprint was published on January 28th, 2021. See the published version at https://doi.org/10.1186/s40360-021-00473-2.

Abstract

Background: Hormonal *receptor positive* (HR+) breast cancer is the most commonly diagnosed molecular subtype of *breast cancer;* which showed good response to doxorubicin (DOX)-based chemotherapy. Eugenol (EUG) and astaxanthin (AST) are natural compounds with proved epigenetic and immunomodulatory effects in several cancer cell lines. This study has been initiated to improve the cytotoxic activity and reduce resistance of DOX through combination with EUG and AST in MCF7 cells.

Methods: Cytotoxic activity of DOX alone and combined with either 1mM EUG or 40μM AST was performed using sulphorhodamine-B assay in MCF7 cells. Global histones acetylation and some immunological markers were investigated using ELISA, western blotting and quantitative RT-PCR techniques. Functional assay of multidrug resistance was performed using rhodamine 123 and Hoechst 3342 dyes. Flow cytometry with annexin V and propidium iodide were used to assess the change in cell cycle and apoptosis along with the expression of some differentiation, apoptosis and autophagy proteins.

Results: DOX alone resulted in concentration-dependent cytotoxicity with IC_{50} of 0.5 μM. Both EUG and AST significantly increased DOX cytotoxicity which is manifested as a significant decrease in DOX IC_{50} from 0.5 μM to 0.088 μM with EUG and to 0.06 μM with AST. Combinations of DOX with 1mM EUG or 40 μM AST significantly increased the level of histones acetylation and histone acetyl transferase expression, while reduced the expression of aromatase and epidermal growth factor receptor (EGFR) when compared with 0.25 μM DOX alone. Also both combinations showed higher uptake of rhodamine but lower of Hoechst stains, along with increased the percentage of caspase 3, and decreased the expression of CK7 and LC3BI/II ratio. EUG combination induced IFγ but reduced TNFα causing shifting of cells from G2/M to S and G0/ G1 phases. Combination of DOX with EUG induced apoptosis through the higher BAX/ BCl2 ratio, while with AST was through the increase in caspase 8 expressions.

Conclusion: EUG and AST potentiated the anticancer activity of DOX through epigenetic histones acetylation along with the immunonomodulation of different apoptotic approaches in MCF7 cells.

Background:

According to the most recent Global Cancer Statistics issued in 2018, breast cancer is the most commonly diagnosed cancer among females and the leading cause of cancer death [1]. Hormonal receptor-positive (HR+) breast cancer is the most common molecular subtype of breast cancer and represents about 84% of breast cancer cases [2]. Breast cancer is a heterogenous disease, in which variant molecular features and therapeutic responses were noticed among patients [3]. Epigenetic modifications were amongst the potential players in hormone resistance. De novo and drug induced alterations in DNA methylation, in the promoter regions of genes, have an impact on the initiation and progression of breast cancer [4, 5]. Epigenomic approach through histones acetylation has become a crucial strategy in the way to solve the acquired resistance [6, 7]. The dynamic reaction catalyzed by

histone acetyltransferases (HATs) and histone deacetylases (HDACs) has a role in the stimulation or the suppression of tumor growth and progression [4]. Using a combination of HDAC inhibitor with chemotherapy; causes re-sensitization of resistant breast cancer cells to treatment [8, 9]. In addition, the interaction of breast cancer cells with the surrounding microenvironment via interleukins and growth factors was found to have significant impact on the response to endocrine therapy [10]. Immunological regulatory protein such as tumour necrosis factor (TNF), interferon-γ (IFN-γ) and forkhead box P3 (FOXP3) have shown direct/ indirect effects on cancer cell. They mediate the tumor-stromal cell interaction inducing range of matrix metalloproteinases, cytokines and chemokines to promote the tumor development and response to therapy [11, 12].

Doxorubicin (DOX) is an anthracycline antibiotic with broad spectrum anti-tumour activity against many forms of human tumours. It is one of the most commonly used chemotherapeutic agents in the treatment of HR + breast cancer patients with poor prognostic features [13]. Unfortunately, the optimal clinical usefulness of DOX is usually limited secondary to the development of multidrug resistance phenotype as a major limitation observed in HR + breast cancer treatment [14]. In an attempt to minimize the serious side effects of DOX and to increase its activity, variety of approaches has been investigated using safe and natural compounds [15–17].

Eugenol (EUG) and astaxanthin (AST) are well- known phytochemical which have proven anticancer properties against breast cancer [18–20]. EUG showed versatile pharmacological actions in different types of cancer [21]. It has genoprotective effects against oxidative and methylated DNA damage [22]. Also, it has dose-dependent suppressive and enhancing effects on the immune response in-vitro and in-vivo [23, 24]. AST, a marine derived xanthophyll carotenoid, has shown to target epigenetic modifying enzymes such as DNMTs and HDACs [25, 26]. Several mechanisms have been proposed for AST induced immunological and anti- inflammatory effects including enhancing both cell-mediated and humoral immune responses. It improves IFN-γ and IL-2 secretion, natural killer cell cytotoxic activity and reduces the intracellular oxidative stress [27, 28]. Accordingly, the current study has been initiated to investigate, on mechanism-based, whether the epigenetic and immunomodulatory effects of EUG and AST could enhance the cytotoxic activity and reduce the acquired resistance to DOX therapy in HR + breast cancer cells (MCF7).

Methods:

Drugs and chemicals

DOX, EUG an AST were obtained from Sigma Aldrich Chemical Co. (St. Louis, MO, USA). Each vial of DOX contains one gm powder which was dissolved in DMSO to yield 10 μM then serially diluted in RPMI-1640 medium immediately before use. EUG was obtained in a vial containing 100% pure essential oil. It was dissolved in DMSO and diluted with RPMI-1640 supplemented medium immediately before use. AST was purchased as pink to very dark purple powder stored away from light and dissolved in DMSO to produce stock of 2000 μM. RPMI-1640 Medium, fetal bovine serum, dimethylsulfoxide (DMSO), sodium

bicarbonate, Hoechst 3342 solution 1 mg/ml, and rhodamine 123 were all purchased from Sigma Aldrich Chemical Co. (St. Louis, MO, USA). Trichloroacetic acid (TCA) and Triton X-100 were procured from MP Biochemical (Santa Ana, California, USA). All other chemicals and reagents were from standard analytical grade.

Cells and cell culture:

Human breast cancer cell line (MCF7) used in this study was obtained from the American Type Culture Collection (Manassas, USA). The adherent cells were grown as monolayer in RPMI- 1640 supplemented with 10% fetal bovine serum, 2 mM L-glutamine, 1.5 g/l sodium bicarbonate and 1% penicillin/streptomycin, and incubated at 37 ◻ C in 5% CO2 atmosphere.

Assessment of cytotoxic activity:

Cytotoxicity was determined using sulforhodamine B (SRB) assay as previously described by Skehan et al. [29]. Briefly, exponentially growing cells were seeded in 96-well microtitre plates at an initial density of 5x 10^3/well. After 24 h, cells were incubated with different concentration of EUG (0.125-4 mM), AST (5-80 µM), DOX (0.0625-1 µM) alone and DOX combined with 1mM EUG, or 40 µM AST. For each concentration, three wells were used and incubation was continued for another 48 h. A control wells containing, vehicles DMSO (1 % v/v) were used and the cells were incubated in a humidified, 5% CO2 atmosphere at 37 ◻ C for 48 h. Cells were fixed with 10% trichloroacetic acid for 1 h at 4 ◻ C and stained with 0.4% SRB for 30 min. The wells were then washed four times with 1% acetic acid, air-dried and the dye was solubilized with 10 mM Tris base (pH 10.5). The optical density (O.D.) was measured spectrophotometrically at 570 nm with the microplate reader (Tecan Sunrise™, Ma¨nnedorf, Switzerland). The experiment was repeated in three independent times. IC_{50} values (the concentration of DOX required to produce 50% inhibition of cell growth) were calculated using sigmoidal dose response curve-fitting models (Graphpad Prizm Software, version 5, GraphPad Software, Inc. Avenida de la Playa La Jolla, USA). The combination index was calculated using CombuSyn software (ComboSyn, Inc., Paramus, NJ., USA).

Cell cycle and apoptosis analysis with flow cytometry:

Control and treated MCF7 cell pellets were stained with DAPI/Triton X-100 staining solution for cell cycle analysis and with propidium iodide for apoptosis analysis [30]. A flow cytometer (Becton and Dickinson San Jose, CA., USA) equipped with electronic doublet-discrimination capability was used to detect stained nuclei and emitted fluorescent light primarily at wavelengths between 580 and 650 nm. The FACscan fluroscence 2 (FL2) detector equipped with a 585/42 band pass filter was used to analyze light emitted between 564 and 606 nm.

RNA extraction, cDNA synthesis and real time PCR:

Total RNA was extracted from control and treated cell pellets with total RNA purification kit (Direct-Zol RNA Kit, Zymo Research, Germany). cDNA synthesis was performed according to the manufacturer's instructions using Revert Aid First Strand cDNA synthesis kit (ThermoFisher, UK). Quantitative real time PCR was conducted according to manufacturer's instructions by Applied Biosystems syber green PCR master mix (USA). Reverse and forward sequences of primers genes encoding for mRNA transcript of TNFα, IFNγ, FOXP3, BAX, BCl2 and caspase 8 genes were designed by NCBI- NIH tool and the sequences were summarized in table (1). Fold change of genes expression ($2^{-\Delta\Delta Ct}$) was calculated after normalization to housekeeping gene (β-actin) and genes expression in control samples.

Table (1): Primers for qRT- PCR

Gene	Forward Primer	Reverse Primer
TNFα	CTGAACTTCGGGGTGATCG	GCTTGGTGGTTTGCTACGAC
IFNγ	ACTGTCGCCAGCAGCTAAAA	TATTGCAGGCAGGACAACCA
FOXP3	CCCAGGAAAGACAGCAACCTT	TTCTCACAACCAGGCCACTTG
BAX	GCCCTTTTGCTTCAGGGTTT	TCCAATGTCCAGCCTTTG
BCl2	CGGAGGCTGGGATGCCTTTG	TTTGGGGCAGGCATGTTGAC
caspase 8	TTCTCCCTACAGGGTCATGC	GCAGGCTCAAGTCATCTTCC
β- actin	CCAGAGCAAGAGAGGTATCC	CTGTGGTGGTGAAGCTGTAG

SDS-polyacrylamide gel electrophoresis and immunoblot analysis:

Control and treated cells were harvested, washed twice with ice-cold phosphate buffered saline, centifuged and pelleted at 1200 r/min for 5 min. The cell pellets were then lysed in lysis buffer containing 150 mM sodium chloride, 10 mM Tris, 0.2% Triton X-100, 0.3% NP-40, 0.2 mM sodium vanadiumoxide and protease inhibitor cocktail, pH 7.7. The supernatants were collected after centrifugation at 14,000 r/min for 15 min at 4 □ C, and the protein content was determined by the Bradford method [31]. Aliquots of protein supernatants containing equal amounts of protein and sodium dodecyl sulphate (SDS)-reducing buffer were boiled for 5 min, electrophoresed on SDS-polyacrylamide gels and transferred to polyvinylidene difluoride membranes. The membranes were blocked with 5% non-fat drymilk and probed with specific primary antibodies of monoclonal antihuman aromatase (Biospes, Aachen, Germany), EGFR (Sigma Aldrich, USA), CK7 (Bioss, Boston, USA) and LC3B (Invitrogen, USA) antibodies followed by incubation with peroxidase-conjugated secondary antibodies. The blots were developed with Amersham

ECL Western Blotting Detection Reagents (GE Healthcare, Amersham Place, Little Chalfont, UK) according to themanufacturer's protocol. The blots were quantified by Scion image software (Scion Corporation, version 0.4.0.3, Maryland, USA) and protein loading was corrected for β-actin as loading control.

Histones extraction and the determination of global H3 and H4 acetylation:

Cell pellets were suspended in triton extraction buffer (0.5% Triton in phosphate buffered saline, 2 mM phenylmethylsulfonyl fluoride and 0.02% NaN3), and lysed on ice for 10 minutes with gentle stirring. After centrifugation, cell lysate was transferred to a new vial and the residual cells were resuspended in the extraction buffer (0.5N HCl + 10% glycerol) and incubated on ice for 30 minutes. The supernatant fraction was taken to a new vial and 8 volumes of acetone was added and left at − 20 °C overnight. The Protein concentration was quantified in the remaining dry pellet by Coomassie protein assay kit following Bradford method[27]. The EpiQuik™ Total Histone H3 and H4 Acetylation Detection Fast Kits (Epigentek, Farmingdale, NY, USA) were used according to the manufacturer` protocol. The global content of acetylated histones in treated samples was calculated from the protein calibration curve in ng/ total histones protein, and then the % of histones acetylation in was calculated normalized to the level of acetylated histones in untreated control.

Enzyme-linked immunosorbent assay for caspase 3:

The concentration of executioner caspase 3 active subunit was measured in the lysate of MCF-7 cells using the Quantikine human active caspase-3 immunoassay kit (R&D system, Minneapolis, MN, USA). The amount of caspase-3 was calculated from a standard curve, and the results are presented as relative % of active caspase-3 to untreated control.

Determination of the activity of multidrug resistance (MDR) via rhodamine-123 and Hoechst dyes.

Rhodamine-123 and Hoechst 3342 dyes are substrates for MDR genes and the proteins codified by these genes including p-glycoprotein (P-gp), MDR associated protein, breast cancer resistant protein and lung-resistant related protein. Accumulation of Rhodamine-123 and Hoechst dyes in the cells is inversely related to MDR activity [32]. In brief, adherent control and treated cells were incubated with 5.25 μM of Rhodamine 123 and 5 ug/ml of Hoechst 33342 dye for 30 min at 37 □ C in a 5% CO2 incubator. After incubation, cells were washed, scrapper collected, re-suspended and physically lysed in distilled water for immediate fluorescence analysis. Cellular uptake of Rhodamine 123 was detected at excitation 485 nm and emission 535 nm, while cellular uptake of Hoechst 3342 was detected at excitation 360 nm and

emission 450 nm using florescence spectroscopy (Kontron SFM25, Tresser Instruments, Rossdorf, Germany).

Statistical analysis:

All data are expressed as mean ± SD of three separate experiments, each performed in triplicates. Differences between groups were tested for statistical significance using one-way analysis of variance (ANOVA) followed by Dunnette for comparing all means with control in the SRB cytotoxicity study and Tukey-kramer for multiple comparison in rest of the experiments. A student t-test was used for comparison between the mean in DOX alone and the corresponding mean in DOX combined with either EUG or AST in SRB cytotoxicity study. Nonparametric ANOVA was carried out for comparison between three blots of Western blotting using the Kruskal–Willis test. The 0.05 level of probability was used as the criterion of significance using GraphPad InStat, version 4.0 (GraphPad, San Diego, California, USA).

Results

Effect of EUG or AST on DOX Cytotoxicity in MCF-7 cells.

Figure (1) shows the effects of EUG (A) and AST (B) on the survival of MCF7 cells after 48 hr incubation period. EUG and AST caused a concentration-dependent cell death. The IC50 recorded for EUG was 0.74 mM, and for AST was 33.8 µM. The concentration that produced significant decrease of survival in MCF7 for EUG and AST was the nearest concentration above the IC_{50} which found to be 1 mM of EUG and 40 µM of AST. Figures 1C and 1D showed the effects of 1 mM EUG (C) and 40 µM AST (D) combined with various concentrations (0.0625–1 µM) of DOX for 48 h on the survival of MCF7 cells. DOX alone resulted in concentration-dependent cytotoxicity with IC_{50} of 0.5 µM. Both EUG and AST significantly increased DOX cytotoxicity manifested as a significant decrease in DOX IC_{50} from 0.5 µM to 0.088 with EUG (C) and to 0.06 µM with AST (D). The combination index-fraction affected graph was drawn and presented in figures (1E) and (1F) for EUG and AST, respectively. The combination of 0.25 µM DOX + 1 mM EUG caused reduction in the cell growth of MCF7 by a fraction of 0.73, and a synergistic combination index of 0.44 (Fig. 1E). The combination of 0.25 µM DOX + 40 µM AST caused reduction in the cell growth of MCF7 by a fraction of 0.61, and a synergistic combination index of 0.63 (Fig. 1E).

The effect of EUG and AST on the level of histones acetylation in DOX treated MCF7 cells.

Significant increase in H3 acetylation was shown only with EUG treatment compared with control (Fig. 2A). The combination of DOX with EUG caused a significant increase in both H3 and H4 histones acetylation, while with AST it caused only a significant increase in H3 histone acetylation, compared with DOX alone (Fig. 2A). Significant increase in H4 histone acetylation was demonstrated in both EUG and AST combination compared with their corresponding single treatment of each (Fig. 2A). HAT protein expression was significantly increased in DOX, EUG and AST treated cells compared with control (Fig. 2B

and 2C). Also, a significant overexpression of HAT was demonstrated in cells treated with DOX combined with EUG and AST compared with DOX, EUG and AST each alone (Figs. 2B and 2C).

Immunological modulation of EUG and AST to DOX activity on FOXP3, IFNγ, TNFα, aromatase and EGFR expression in MCF7 cells.

In figure (3A), single treatment with DOX and EUG caused a significant decrease in FOXP3 and TNFα, but increased mRNA expression of IFNγ compared with control. Single treatment with AST caused significant mRNA overexpression of FOXP3, IFNγ and TNFα compared with control. EUG combination caused a significant increase in IFNγ but it decreased TNFα compared with DOX. AST plus DOX combination caused a significant decrease in FOXP3 expression compared with AST alone and also caused a significant decrease in IFNγ expression compared with single DOX and AST. The expression of TNFα in AST plus DOX was higher than in DOX but lower than in AST alone. In figures (3B and 3C), single treatment with DOX, EUG and AST caused significant decrease in aromatase and EGFR protein expression compared with control. DOX combinations with EUG and AST caused further decrease in aromatase and EGFR protein expression compared with single treatment with DOX, EUG and AST.

EUG and AST modulated the multidrug resistance of MCF7 cells to DOX.

DOX treated cells had significant higher uptake of rhodamine 123 (Fig. 4A), but lower uptake of hoechst3342 (Fig. 4B), compared with control. EUG and AST treated cells had significant higher uptake of rhodamine 123 (Fig. 4A), and hoechst3342 (Fig. 5B), compared with control. The combination of DOX with EUG resulted in significant higher uptake of rhodamine123 compared with single treatment with DOX and EUG (Fig. 4A). The combination of DOX with AST resulted in significant higher uptake of rhodamine123 compared with single treatment with DOX but lower uptake of rhodamine123 compared with single treatment with AST (Fig. 4A). Cells treated with EUG and AST combination showed lower Hoechst 3342 uptake than cells treated with DOX, but higher Hoechst 3342 uptake than cells treated with single EUG or AST (Fig. 4B).

Combined treatment of DOX with EUG shifted cells into the G0/ G1 phase of cell cycle and both EUG and AST combinations inhibited the expression of CK7.

Compared with control, ascending accumulation of cells in G0/G1 was observed with EUG, DOX and AST treatment (1.64, 2.01 and 5.87%, respectively). The combination of DOX with EUG resulted in five folds increase in the percentage of cells in G0/G1 (10.99%) compared with cells treated with DOX alone (2.01%). However, no change was observed in the distribution of cells between AST combined with DOX and DOX alone (Fig. 5A). Protein expression of luminal differentiation marker (cytokeratin 7: CK7) was shown to be significantly reduced in MCF7 cells treated with single DOX, EUG and AST compared with control, and further reduction was observed when DOX combined with EUG and AST compared with single DOX, EUG and AST (Fig. 5B).

EUG induced intrinsic apoptosis through BAX/ BCl2 while AST induced extrinsic apoptosis through caspase 8 and both activated caspase 3 in early apoptosis and reduced LC3B expression.

The percentage of active caspase 3 subunit was shown to be significantly reduced in DOX treated cells, while significantly induced in EUG treated cells, compared with control. Combination of EUG with DOX significantly induced capase 3% compared with DOX alone. While combination of AST with DOX significantly induced capase 3% compared with DOX and AST alone (Fig. 6A). Single treatment with EUG showed significant overexpression of BAX/ BCl2 ratio, but downexpression of caspase 8, compared with control. On the contrary, AST showed significant downexpression of BAX/ BCl2 ratio, but overexpression of caspase 8, compared with control. Cells treated with EUG combination revealed significant higher level of BAX/ BCl2 ratio but lower level caspase 8 compared with cell treated with DOX alone. Cells treated with EUG combination revealed significant lower level of BAX/ BCl2 ratio when compared with cells treated with EUG alone. When AST combination compared with DOX, significant lower level of BAX/ BCl2 ratio but significant higher level of caspase 8 was revealed. The level of caspase 8 mRNA expression in cells treated with AST combination was lower than in cells treated with AST alone (Fig. 6B). EUG and AST combination caused early apoptosis to 1.25% of cells compared with 0.87% of cells treated with DOX alone (Fig. 6C). The protein expression of autophagic marker (LC3BII/I ratio) was shown to be significantly reduced in MCF7 cells treated with single DOX, EUG and AST compared with control, and further reduction was observed when EUG and AST combinations compared with single DOX, EUG and AST (Fig. 6D).

Discussion

DOX is among the most commonly used anticancer drugs with broad spectrum antitumor activity against several human tumours including breast cancer. Unfortunately, the optimal clinical benefits of DOX are limited secondary to its detrimental cardiomyopathy and the development of MDR [33, 34]. Earlier studies have demonstrated that EUG attenuated DOX-induced genotoxicity and cardiotoxicity [15, 16]. Similarly, AST treatment significantly protected against DOX-induced oxidative and inflammatory insults and downregulated the overactive apoptotic machineries [17]. Therefore, the current study extended such beneficial effects of EUG and AST by testing their combination with DOX in MCF7 to investigate, on mechanism-based, whether EUG and AST could enhance the sensitivity of HR + MCF7 cells to DOX, and if so, whether these effects are linked to MDR-P-gp pathway and/or the non-MDR-epigenetic immunomodulation.

Data presented in the current study showed that EUG and AST induced remarkable enhancement in DOX cytotoxicity in MCF-7 cells manifested as a significant 82% and 88% decrease in the IC_{50}, respectively as compared to DOX alone (Fig. 1). Our results confirmed earlier study which has reported that EUG induced cytotoxic activity against different molecular subtypes of breast cancer cells and induced apoptosis in a p53-independent manner [18]. Using MCF7 cells, Vidhya and Devaraj [35] reported that EUG treatment caused concentration and time-dependent inhibition of growth and proliferation of the cells and

increased the percentage of apoptotic cells and DNA fragmentation through depleting the level of intracellular glutathione and increasing the level of lipid peroxidation.

The current results showed that addition of EUG to DOX-treated cells resulted in shifting MCF-7 cells toward the S and G0/ G1 phases and induced the intrinsic apoptosis through the higher BAX to BCl2 ratio (Fig. 6B). In concordance, DOX induced mitochondrial-dependent apoptosis by down-regulation of Bcl-xL and up-regulation of Bax and caspase-9 expressions in MCF7 cells [36]. In addition, Júnior et al. [37] pointed that EUG induced apoptosis in cancer cells through promoting the production of reactive oxygen species and reducing the mitochondria potential through the upregulation of Bax expression causing the abrogation of cells from the G2/M of phase of cell-cycle. Moreover, the chemo-sensitivity of MCF-7 cells to EUG was found to be mainly mediated through the distortion of mitochondrial membrane integrity with the consequent release of cytochrome-c and lactate dehydrogenase into culture media at EUG concentration more than its effective concentration 50 [19]. Therefore, one can anticipate a synergistic harmony between DOX and EUG in the molecular insights leading to apoptosis. On the other hand, our results revealed that DOX combination with AST induced apoptosis through overexpression of caspase 8, the key enzyme of the extrinsic apoptosis, and there was insignificant change in the distribution of cells through the phases of cell cycle. Under similar experimental condition, Sharifi et al. reported that DOX induced non-significant change in the level of caspase 8 after 24 hour incubation, but significantly increased its level after 48 and 72 hours of incubation [36]. Different modes of AST driving apoptosis when combined with DOX were recently reported [38 and 39]. It has been reported that, the pro-oxidant property of AST was the main force for selective apoptosis MCF7 cells in which growth inhibition was increased in a synergistic pattern rather than normal breast epithelial cells (MCF-10A) [38]. In vivo study concluded that AST caused up-regulation of tumor suppressor p53 gene, potentiating DOX cytotoxicity and apoptosis against mammary tumor cells but accumulating them in the G2/M phase of the cell cycle [39].

Earlier studies confirmed that DOX-treated MCF-7 cell developed varying degrees of resistance depending on the concentration of DOX used [40] and that DOX is a selective P-gp substrate, and induced expression of MDR in tumor cells [41]. Therefore, to test EUG and AST sensitization of MCF7 to DOX treatment, the current study followed two approaches; one through the direct measurement of MDR-Pgp post-translational activity, and the other is non-MDR mediated through the measurement of CK7, LC3B, immunological and epigenetic markers. In this study, the sensitization of MCF7 cells to DOX treatment was investigated by the functional assay of MDR depending on the intracellular accumulation of Rhodamine 123 and Hoechst dyes [42, 43]. Our results showed that treatment with DOX alone caused reduced intracellular Rhodamine 123 accumulation but induced that of Hoeacsht 3342, indicating the basal sensitive nature of our MCF7 cells (Fig. 4B). Combined use of EUG or AST with DOX induced higher uptake of Rhodamine123, but lower of Hoechst 3342 than DOX alone, indicating the switch on induction of the P-gp activity upon combination treatment. Alterations of mitochondrial membrane potential and intracellular ATP level by EUG [44, 19] and AST were reported [45, 46].

In our study, the combination of DOX with both EUG and AST significantly decreased CK7 expression. It is well known that cells with positive expression of CK7 exhibited resistance to DOX treatment [47, 48]. The immunomodulation potency of EUG and AST on the differentiation of mesenchymal stem cells which affect therapy applications was reported [49, 50]. For further elucidation of the non-MDR directed EUG and AST sensitization to DOX anticancer activity in MCF7 cells, we investigated the effect of DOX alone and combined with EUG or AST on EGFR and aromatase expression. Our results showed that EUG and AST alone induced mild anti-EGFR effect. However, after combined treatment with DOX, EUG or AST, caused marked reduction in EGFR and aromatase proteins expression. Our results are consistent with previous studies which reported that DOX showed resistance secondary to the increase of EGFR number [51], and that combination of DOX with anti-EGFR therapy enhanced DOX effects against EGFR overexpressed tumor xenografts [52]. The ability of EUG to block HER2/PI3K-AKT signalling in breast precancerous lesions was reported [53]. In cervical cancer cells, AST reduced the expression of EGFR and interfere with EGF binding, thereby inducing apoptosis [54]. Aromatase and estrogen receptor α (ER α) are two key proteins which are responsible for the proliferation of MCF7 cells [55]. Our results showed a significant inhibitory activity of DOX against aromatase enzyme. Pritchard et al. showed that DOX induced changes on estrogen signaling relevant to its therapeutic efficacy [13]. However, the presence of physiological estrogen levels will reverse DOX cytotoxic effect in breast cancer cells [13]. The anti-oxidant and anti-inflammatory activities of EUG and AST were suggested to contribute in their anti-aromatase effects. The idea was exported from the well- known aromatase inhibitor (exemestane) which showed non-estrogenic chemopreventive activity through its anti-inflammatory and reactive oxygen species scavenging properties [56]. Red clover flowers (from which EUG was extracted) were found to inhibit aromatase at low concentrations, while they had estrogenic activity at high concentrations [57]. Moreover, we suggest that the known anti-hyperlipidemic effect of AST [58] may also contribute in its aromatase inhibitory activity [59]. Especially there is a classical correlation between ER-positive breast cancers and adipose tissue expression of aromatase, which is considered a local source of estrogens [60].

Autophagy is the main reason for acquired resistance phenotype in ER + breast cancer, and its molecular target LC3B is found to be highly expressed in the breast cancer tissues [61]. Data presented in the current study showed that the expression of LC3BI and II was vanished in cells treated with DOX combined with EUG or AST as compared to each alone (Fig. 6D). In colorectal cancer cells, EUG was identified as pro-autophagic compound [62], where the active fraction of clove (oleanonic acid and eugenol) increased LC3B I and II and Beclin-1 protein expression. AST modulates the signaling pathways that regulate autophagy [63], either by stimulation as shown in an experimental model of non-alcoholic fatty liver disease [64], or by inhibition as shown in the pancreas by inhibiting the JAK/STAT3 pathway [65]. Also the anti-oxidant and reactive oxygen scavengining activities of EUG [66] and AST [67] during DOX treatment may explain for the classical autophagic inhibition usually observed in that context with other anti-oxidant compounds [68].

Under our experimental condition; the epigenetic potential of EUG and AST was evaluated, and it was found that EUG alone and the combinations of DOX with 1 mM EUG or 40 μM AST significantly induced the level of global histones acetylation along with increasing the protein expression of histone acetyl

transferase (Figs. 2A, 2B and 2C). This histone deacetylase inhibition activity observed with EUG illustrates its proautophagic effect and intrinsic apoptotic cell death. On the same way, most of histone deacetylase inhibitors can induce mitochondria-mediated apoptosis and provoke autophagy-induced caspase-independent cell death [69, 70]. The inhibitory effect of AST on histone deacetylase 9 expressions was observed [71]. Combination of DOX with histone deacetylase inhibitors promoted DOX-induced apoptosis through a mechanism that involved induction of tumor suppressor gene PTEN which is the major negative regulator of the PI3K/Akt cellular survival pathway [72]. According to that, the proven induction of H3 and H4 histone acetylation by EUG and AST was suggested to contribute in the DOX synergistic cell death observed in this study.

In the present study, exposure of MCF7 cells to either DOX or EUG alone significantly decreased expression of FOXP3 and TNFα and increased expression of IFNγ, while AST caused overexpression of the three genes (Fig. 3A). DOX combined with EUG significantly increased IFNγ expression and decreased TNFα expression when compared with DOX alone. The vice versa was observed when AST combined with DOX where a significant reduction in IFNγ expression accompanied with TNFα overexpression in comparison with DOX alone. Both EUG and AST combinations showed no change in FOXP3 expression compared with single treatment with DOX. Moreover, DOX induced a remarkable increase in Foxp3 protein in MCF7 cells that was associated with the phosphorylation of p53 [73]. Recent study suggested that the antitumor effect of EUG was secondary to its regulatory action on the production of inflammatory mediators from macrophages Barboza et al. [24]. EUG reduced TNF-α and IL-1β as well as the NF-κB, ERK1/2, and p38 MAPK signaling pathways [74]. EUG exhibited synergistic effect when combined with gemcitabine by downregulating the expression of Bcl-2, COX-2 and IL1-β [75]. It has been also reported that EUG induced downregulation of TNF-α in LPS-activated macrophages, which was associated with antigenotoxic activity when DNA damage was induced with DOX [15]. Additionally, it was reported that EUG synergistically increased cisplatin cytotoxicity against triple negative breast cancer through the inhibition of NF-κB signalling pathway, p50 and p65 subunits phosphorylation, and IL-6 and IL-8 downregulation [76]. In tumor environment, it has been reported that AST decreased the amount of inflammatory markers such as TNF-α, IL-6, and IFNγ via NFκ-B inhibition [77]. In mouse breast cancer model, AST treatment caused higher levels of apoptotic cancer cells and [78], promoted early check and elimination of cells undergoing malignant transformation by activating immune surveillance [79] and prevented cancer cell growth in cells by boosting immune detection [80].

Conclusions

In conclusion, EUG and AST enhanced the cytotoxic activity of DOX through two different apoptotic approaches, mainly through the non-MDR pathway of histones acetylation and immunonomodulation in hormone receptor positive breast cancer cells. EUG and AST significantly synergize DOX cytotoxicity in HR + breast cancer cells. Combined use of EUG or AST with DOX significantly increased histones acetylation, Rhodamine123 uptake and caspase-3%, and decreased protein expression of aromatase, EGFR, CK7 and LC3B. DOX combined with EUG significantly increased IFNγ and decreased TNFα but vice versa was observed when AST combined with DOX where a significant reduction in IFNγ expression

accompanied with TNFα overexpression was shown in comparison with DOX alone. Both EUG and AST have non-significant effect on FOXP3 mRNA expression. EUG combination caused shifting of cells from G2/M to S and G0/ G1 phases, whereas AST combination caused non-significant change. EUG combination induced apoptosis through increasing BAX/ BCl2 ratio, while AST combination was through increasing caspase- 8 expression. Our results warrant a detailed mechanistic in-vivo study to confirm the chemosensitizing effects of EUG and AST to minimize the therapeutic dose of DOX with the consequent decrease in its organ toxicity.

Abbreviations

DOX, doxorubicin; EUG, eugenol; AST, astaxanthin; HR+, hormonal receptor positive; EGFR, epidermal growth factor receptor, HAT, acetyltransferase; HDAC, histone deacetylase, TNF, tumour necrosis factor; IFN-γ, interferon-γ, FOXP3, forkhead box P3.

Declarations

Ethics approval and consent to participate:

This article does not contain any studies with human or animal subjects performed by the authors.

Consent to publish

Not applicable.

Availability of data and materials

All data analyzed in this study is available from the corresponding author on reasonable request.

Competing interest

The authors declared that have no competing interest.

Funding

This research is supported from the annual research fund by National Cancer Institute, Cairo University (No.19/20)

Authors' contributions:

MAF and HFH designed and performed the experimental work and analysed the data. MMS shared in analysis and interpretation of the data. EAH shared in analysis and interpretation of the data and AMO suggested the research problem and designed the experimental work. All authors contributed in writing and revising of the manuscript and approved it.

Acknowledgements

Authors are grateful to Dr. Mohamed M. Hafez Prof. of Virology & Immunology for facilitating the use of real time- PCR.

References

1. Bray F, Ferlay J, Soerjomataram I, Siegel RL, Torre LA, Jemal A. Global cancer statistics 2018: GLOBOCAN estimates of incidence and mortality worldwide for 36 cancers in 185 countries. CA Cancer J Clin. 2018;68(6):394-424. doi: 10.3322/caac.21492.
2. American Cancer Society. Breast Cancer Facts & Figures 2019-2020. Atlanta: American Cancer Society, Inc. 2019
3. Turashvili G, Brogi E. Tumor Heterogeneity in Breast Cancer. Front Med (Lausanne). 2017;4:227. doi:10.3389/fmed.2017.00227
4. Abdel-Hafiz HA, Horwitz KB. Role of epigenetic modifications in luminal breast cancer. Epigenomics. 2015;7(5):847–862. doi:10.2217/epi.15.10
5. Wang Q, Gun M, Hong XY. Induced Tamoxifen Resistance is Mediated by Increased Methylation of E-Cadherin in Estrogen Receptor-Expressing Breast Cancer Cells. Sci Rep. 2019;9(1):14140. doi:10.1038/s41598-019-50749-1
6. Connolly R, Stearns V. Epigenetics as a therapeutic target in breast cancer. J Mammary Gland Biol Neoplasia. 2012;17(3-4):191–204. doi:10.1007/s10911-012-9263-3
7. Feng Q, Zhang Z, Shea MJ, et al. An epigenomic approach to therapy for tamoxifen-resistant breast cancer. Cell Res. 2014;24(7):809–819. doi:10.1038/cr.2014.71
8. Sandhu R, Rivenbark AG, Coleman WB. Enhancement of chemotherapeutic efficacy in hypermethylator breast cancer cells through targeted and pharmacologic inhibition of DNMT3b. Breast Cancer Res Treat. 2012;131(2):385–399. doi:10.1007/s10549-011-1409-2
9. Li, J., Hao, D., Wang, L. et al. Epigenetic targeting drugs potentiate chemotherapeutic effects in solid tumor therapy. Sci Rep 7, 4035 (2017). doi:10.1038/s41598-017-04406-0
10. Segovia-Mendoza M, Morales-Montor J. Immune tumor microenvironment in breast cancer and the participation of estrogen and its receptors in cancer physiopathology. Front Immunol. 2019;10:348. doi:10.3389/fimmu.2019.00348.
11. Esquivel-Velázquez M, Ostoa-Saloma P, Palacios-Arreola MI, Nava-Castro KE, Castro JI, Morales-Montor J. The role of cytokines in breast cancer development and progression. J Interferon Cytokine Res. 2015;35(1):1–16. doi:10.1089/jir.2014.0026
12. Soysal SD, Tzankov A, Muenst SE. Role of the Tumor Microenvironment in Breast Cancer. Pathobiology. 2015;82(3-4):142–152. doi:10.1159/000430499
13. Pritchard JE, Dillon PM, Conaway MR, Silva CM, Parsons SJ. A mechanistic study of the effect of doxorubicin/adriamycin on the estrogen response in a breast cancer model. Oncology.

2012;83(6):305–320. doi:10.1159/000341394.

14. Ponnusamy L, Mahalingaiah PKS, Singh KP. Treatment schedule and estrogen receptor-status influence acquisition of doxorubicin resistance in breast cancer cells. Eur J Pharm Sci. 2017;104:424–433. doi:10.1016/j.ejps.2017.04.020
15. M. de Paula Porto, G. N. Da Silva, B. C. O. Luperini et al., “Citral and eugenol modulate DNA damage and proinflammatory mediator genes in murine peritoneal macrophages,” Molecular Biology Reports, vol. 41, no. 11, pp. 7043– 7051, 2014.
16. Fouad AA, Yacoubi MT. Mechanisms underlying the protective effect of eugenol in rats with acute doxorubicin cardiotoxicity. Arch Pharm Res. 2011;34(5):821-828. doi:10.1007/s12272-011-0516-2
17. El-Agamy SE, Abdel-Aziz AK, Wahdan S, Esmat A, Azab SS. Astaxanthin Ameliorates Doxorubicin-Induced Cognitive Impairment (Chemobrain) in Experimental Rat Model: Impact on Oxidative, Inflammatory, and Apoptotic Machineries. Mol Neurobiol. 2018;55(7):5727-5740. doi:10.1007/s12035-017-0797-7
18. Al-Sharif, I., Remmal, A. & Aboussekhra, A. Eugenol triggers apoptosis in breast cancer cells through E2F1/survivin down-regulation. BMC Cancer 13, 600 (2013). doi:10.1186/1471-2407-13-600
19. Al Wafai R, El-Rabih W, Katerji M, et al. Chemosensitivity of MCF-7 cells to eugenol: release of cytochrome-c and lactate dehydrogenase. Sci Rep. 2017;7:43730. doi:10.1038/srep43730
20. McCall B, McPartland CK, Moore R, Frank-Kamenetskii A, Booth BW. Effects of Astaxanthin on the Proliferation and Migration of Breast Cancer Cells In Vitro. Antioxidants (Basel). 2018;7(10):135. doi:10.3390/antiox7100135
21. Pramod, K., Ansari, S. H., & Ali, J. (2010). Eugenol: A Natural Compound with Versatile Pharmacological Actions. Natural Product Communications. doi:10.1177/1934578X1000501236
22. Thapa D, Richardson AJ, Zweifel B, Wallace RJ, Gratz SW. Genoprotective Effects of Essential Oil Compounds Against Oxidative and Methylated DNA Damage in Human Colon Cancer Cells. J Food Sci. 2019;84(7):1979–1985. doi:10.1111/1750-3841.14665
23. Rodrigues TG, Fernandes A Jr, Sousa JP, Bastos JK, Sforcin JM. In vitro and in vivo effects of clove on pro-inflammatory cytokines production by macrophages. Nat Prod Res. 2009;23(4):319–326. doi:10.1080/14786410802242679
24. Barboza JN, da Silva Maia Bezerra Filho C, Silva RO, Medeiros JVR, de Sousa DP. An Overview on the Anti-inflammatory Potential and Antioxidant Profile of Eugenol. Oxid Med Cell Longev. 2018;2018:3957262. doi:10.1155/2018/3957262
25. Li R, Wu H, Zhuo WW, et al. Astaxanthin Normalizes Epigenetic Modifications of Bovine Somatic Cell Cloned Embryos and Decreases the Generation of Lipid Peroxidation. Reprod Domest Anim. 2015;50(5):793–799. doi:10.1111/rda.12589.
26. Yang Y, Fuentes F, Shu L, et al. Epigenetic CpG Methylation of the Promoter and Reactivation of the Expression of GSTP1 by Astaxanthin in Human Prostate LNCaP Cells. AAPS J. 2017;19(2):421–430. doi:10.1208/s12248-016-0016-x.

27. Park JS, Chyun JH, Kim YK, Line LL, Chew BP. Astaxanthin decreased oxidative stress and inflammation and enhanced immune response in humans. Nutr Metab (Lond). 2010;7:18. doi:10.1186/1743-7075-7-18
28. Lin KH, Lin KC, Lu WJ, Thomas PA, Jayakumar T, Sheu JR. Astaxanthin, a Carotenoid, Stimulates Immune Responses by Enhancing IFN-γ and IL-2 Secretion in Primary Cultured Lymphocytes in Vitro and ex Vivo. Int J Mol Sci. 2015;17(1):44. doi:10.3390/ijms17010044
29. Skehan P, Storeng R, Scudiero D, et al. New colorimetric cytotoxicity assay for anticancer-drug screening. J Natl Cancer Inst. 1990;82(13):1107–1112. doi:10.1093/jnci/82.13.1107.
30. Pozarowski P, Darzynkiewicz Z. Analysis of cell cycle by flow cytometry. Methods Mol Biol. 2004;281:301-311. doi:10.1385/1-59259-811-0:301
31. Bradford MM. A rapid and sensitive method for the quantitation of microgram quantities of protein utilizing the principle of protein-dye binding, j. Anal Biochem. 1976;72:248–54. doi: 10.1016/0003-2697(76)90527-3. 11.
32. Sayed-Ahmed, M M. 2007. Multi drug resistance to cancer chemotherapy: Genes involved and blockers. Saudi Pharmaceutical Journal, 15, 161-175.
33. Sayed-Ahmed MM, Al-Shabanah OA, Hafez MM, Aleisa AM, Al-Rejaie SS. Inhibition of gene expression of heart fatty acid binding protein and organic cation/carnitine transporter in doxorubicin cardiomyopathic rat model. Eur J Pharmacol. 2010, 12; 640(1-3): 143-9.
34. Christowitz, C., Davis, T., Isaacs, A. et al. Mechanisms of doxorubicin-induced drug resistance and drug resistant tumour growth in a murine breast tumour model. BMC Cancer 19, 757 (2019). https://doi.org/10.1186/s12885-019-5939-z
35. Vidhya N, Devaraj SN. Induction of apoptosis by eugenol in human breast cancer cells. Indian J Exp Biol. 2011;49(11):871-878.
36. Sharifi S, Barar J, Hejazi MS, Samadi N. Doxorubicin Changes Bax /Bcl-xL Ratio, Caspase-8 and 9 in Breast Cancer Cells. Adv Pharm Bull. 2015;5(3):351-359. doi:10.15171/apb.2015.049
37. Júnior PL, Câmara DA, Costa AS, et al. Apoptotic effect of eugenol envolves G2/M phase abrogation accompanied by mitochondrial damage and clastogenic effect on cancer cell in vitro. Phytomedicine. 2016;23(7):725-735. doi:10.1016/j.phymed.2016.03.014
38. Vijay K, Sowmya PR, Arathi BP, et al. Low-dose doxorubicin with carotenoids selectively alters redox status and upregulates oxidative stress-mediated apoptosis in breast cancer cells. Food Chem Toxicol. 2018;118:675-690. doi:10.1016/j.fct.2018.06.027
39. AlQahtani A A, Osman A M, Al-Kreathy H M, Al-harthy S E, Al-malky H S, AL Nasser M S, Kamel F O, Alaama M N, Damanhouri Z A, 2019. Chemosensitizing effects of marine astaxanthin on the anti-cancer activity of doxorubicin in tumor bearing mice. Int. J. Cancer Res., 15: 1-8.
40. Trebunova M, Laputkova G, Slaba E, Lacjakova K, Verebova A. Effects of docetaxel, doxorubicin and cyclophosphamide on human breast cancer cell line MCF-7. Anticancer Res. 2012;32(7):2849-2854.
41. Gustafson DL, Long ME. Alterations in P-glycoprotein expression in mouse tissues by doxorubicin: implications for pharmacokinetics in multiple dosing regimens. Chem Biol Interact. 2001 Oct 25;

138(1):43-57.

42. Lahmy S, Viallet P, Salmon JM. Is reduced accumulation of Hoechst 33342 in multidrug resistant cells related to P-glycoprotein activity?. Cytometry. 1995;19(2):126-133. doi:10.1002/cyto.990190207
43. van der Sandt IC, Blom-Roosemalen MC, de Boer AG, Breimer DD. Specificity of doxorubicin versus rhodamine-123 in assessing P-glycoprotein functionality in the LLC-PK1, LLC-PK1:MDR1 and Caco-2 cell lines. Eur J Pharm Sci. 2000;11(3):207-214. doi:10.1016/s0928-0987(00)00097-x
44. Yi JL, Shi S, Shen YL, et al. Myricetin and methyl eugenol combination enhances the anticancer activity, cell cycle arrest and apoptosis induction of cis-platin against HeLa cervical cancer cell lines. Int J Clin Exp Pathol. 2015;8(2):1116-1127.
45. Lu YP, Liu SY, Sun H, Wu XM, Li JJ, Zhu L. Neuroprotective effect of astaxanthin on H(2)O(2)-induced neurotoxicity in vitro and on focal cerebral ischemia in vivo. Brain Res. 2010;1360:40-48. doi:10.1016/j.brainres.2010.09.016
46. Kim SH, Lim JW, Kim H. Astaxanthin Inhibits Mitochondrial Dysfunction and Interleukin-8 Expression in Helicobacter pylori-Infected Gastric Epithelial Cells. Nutrients. 2018;10(9):1320. doi:10.3390/nu10091320
47. Anderson JM, Heindl LM, Bauman PA, Ludi CW, Dalton WS, Cress AE. Cytokeratin expression results in a drug-resistant phenotype to six different chemotherapeutic agents. Clin Cancer Res. 1996;2(1):97-105.
48. Hsiao YL, Hsieh TZ, Liou CJ, et al. Characterization of protein marker expression, tumorigenicity, and doxorubicin chemoresistance in two new canine mammary tumor cell lines. BMC Vet Res. 2014;10:229. doi:10.1186/s12917-014-0229-0
49. Yazdani M., BidmeshkipourA., & SisakhtnezhadS. (2018). Evaluating the Effect of Eugenol on the Expression of Genes Involved in the Immunomodulatoty Potency of Mouse Mesenchymal Stem Cells In Vitro. Journal of Cell and Molecular Research, 10(1), 1-10. https://doi.org/10.22067/jcmr.v10i1.70380
50. Wang M, Zhang J, Song X, et al. Astaxanthin ameliorates lung fibrosis in vivo and in vitro by preventing transdifferentiation, inhibiting proliferation, and promoting apoptosis of activated cells. Food Chem Toxicol. 2013;56:450-458. doi:10.1016/j.fct.2013.03.004
51. Kwok TT, Sutherland RM. Epidermal growth factor reduces resistance to doxorubicin. Int J Cancer. 1991;49(1):73-76. doi:10.1002/ijc.2910490114.
52. Baselga J, Norton L, Masui H, et al. Antitumor effects of doxorubicin in combination with anti-epidermal growth factor receptor monoclonal antibodies. J Natl Cancer Inst. 1993;85(16):1327-1333. doi:10.1093/jnci/85.16.1327
53. Ma M, Ma Y, Zhang GJ, et al. Eugenol alleviated breast precancerous lesions through HER2/PI3K-AKT pathway-induced cell apoptosis and S-phase arrest. Oncotarget. 2017;8(34):56296-56310. doi:10.18632/oncotarget.17626

54. Muto Y, Fujii J, Shidoji Y, et al. Growth retardation in human cervical dysplasia-derived cell lines by beta-carotene through down-regulation of epidermal growth factor receptor. Am J Clin Nutr. 1995;62:1535S–1540S.
55. Chan HJ, Petrossian K, Chen S. Structural and functional characterization of aromatase, estrogen receptor, and their genes in endocrine-responsive and -resistant breast cancer cells. J Steroid Biochem Mol Biol. 2016;161:73-83. doi:10.1016/j.jsbmb.2015.07.018
56. Liu H, Talalay P. Relevance of anti-inflammatory and antioxidant activities of exemestane and synergism with sulforaphane for disease prevention. Proc Natl Acad Sci U S A. 2013;110(47):19065-19070. doi:10.1073/pnas.1318247110
57. Almstrup K, Fernández MF, Petersen JH, Olea N, Skakkebaek NE, Leffers H. Dual effects of phytoestrogens result in u-shaped dose-response curves. Environ Health Perspect. 2002;110(8):743-748. doi:10.1289/ehp.02110743
58. Choi HD, Youn YK, Shin WG. Positive effects of astaxanthin on lipid profiles and oxidative stress in overweight subjects. Plant Foods Hum Nutr. 2011;66(4):363-369. doi:10.1007/s11130-011-0258-9
59. Baek AE, Nelson ER. The Contribution of Cholesterol and Its Metabolites to the Pathophysiology of Breast Cancer. Horm Cancer. 2016;7(4):219-228. doi:10.1007/s12672-016-0262-5
60. Wang X, Simpson ER, Brown KA. Aromatase overexpression in dysfunctional adipose tissue links obesity to postmenopausal breast cancer. J Steroid Biochem Mol Biol. 2015; 153:35–44. [PubMed: 26209254]
61. Felzen, V., Hiebel, C., Koziollek-Drechsler, I. et al. Estrogen receptor α regulates non-canonical autophagy that provides stress resistance to neuroblastoma and breast cancer cells and involves BAG3 function. Cell Death Dis 6, e1812 (2015). doi. 10.1038/cddis.2015.181
62. Liu, M., Zhao, G., Zhang, D., An, W., Lai, H., Li, X, Lin, X. (2018). Active fraction of clove induces apoptosis via PI3K/Akt/mTOR-mediated autophagy in human colorectal cancer HCT-116 cells. International Journal of Oncology, 53, 1363-1373. doi. 10.3892/ijo.2018.4465
63. Kim SH, Kim H. Astaxanthin Modulation of Signaling Pathways That Regulate Autophagy. Mar Drugs. 2019;17(10):546. Published 2019 Sep 23. doi:10.3390/md17100546
64. Jia Y, Wu C, Kim J, Kim B, Lee SJ. Astaxanthin reduces hepatic lipid accumulations in high-fat-fed C57BL/6J mice via activation of peroxisome proliferator-activated receptor (PPAR) alpha and inhibition of PPAR gamma and Akt. J Nutr Biochem. 2016;28:9-18. doi:10.1016/j.jnutbio.2015.09.015
65. Zhang, H.; Yang, W.; Li, Y.; Hu, L.; Dai, Y.; Chen, J.; Xu, S.; Xu, X.; Jiang, H. Astaxanthin ameliorates cerulein-induced acute pancreatitis in mice. Int. Immunopharmacol. 2018, 56, 18–28.
66. Gülçin İ. Antioxidant activity of eugenol: a structure-activity relationship study. J Med Food. 2011;14(9):975-985. doi:10.1089/jmf.2010.0197
67. Sztretye, M., Dienes, B., Gönczi, M., Czirják, T., Csernoch, L., Dux, L., Szentesi, P., & Keller-Pintér, A. (2019). Astaxanthin: A Potential Mitochondrial-Targeted Antioxidant Treatment in Diseases and with Aging. Oxidative Medicine and Cellular Longevity, 2019.

68. Underwood BR, Imarisio S, Fleming A, et al. Antioxidants can inhibit basal autophagy and enhance neurodegeneration in models of polyglutamine disease. Hum Mol Genet. 2010;19(17):3413-3429. doi:10.1093/hmg/ddq253
69. Liu YL, Yang PM, Shun CT, Wu MS, Weng JR, Chen CC. Autophagy potentiates the anti-cancer effects of the histone deacetylase inhibitors in hepatocellular carcinoma. Autophagy. 2010 Nov; 6(8):1057-65.
70. Mrakovcic M., Fröhlich L.F. Regulation of HDAC Inhibitor-Triggered Autophagy. SF Onco. Cancer Res. J. 2017;1:2–4.
71. Yang Y, Bae M, Park YK, et al. Histone deacetylase 9 plays a role in the antifibrogenic effect of astaxanthin in hepatic stellate cells. J Nutr Biochem. 2017;40:172-177. doi:10.1016/j.jnutbio.2016.11.003
72. Pan L, Lu J, Wang X, et al. Histone deacetylase inhibitor trichostatin a potentiates doxorubicin-induced apoptosis by up-regulating PTEN expression. Cancer. 2007;109(8):1676-1688. doi:10.1002/cncr.22585
73. Jung DJ, Jin DH, Hong SW, et al. Foxp3 expression in p53-dependent DNA damage responses. J Biol Chem. 2010;285(11):7995-8002. doi:10.1074/jbc.M109.047985
74. J. L. Yeh, J. H. Hsu, Y. S. Hong et al., “Eugenolol and glycerylisoeugenol suppress LPS-induced iNOS expression by downregulating NF-κB AND AP-1 through inhibition of MAPKS and AKT/IκBα signaling pathways in macrophages,” International Journal of Immunopathology and Pharmacology, 2011, 24 (2): 345–356.
75. Hussain, K. Brahmbhatt, A. Priyani, M. Ahmed, T. A. Rizvi, and C. Sharma. Eugenol enhances the chemotherapeutic potential of gemcitabine and induces anticarcinogenic and anti-inflammatory activity in human cervical cancer cells. Cancer Biotherapy and Radiopharmaceuticals, 2011, 26 (5): 519–527.
76. S. S. Islam, I. Al-Sharif, A. Sultan, A. Al-Mazrou, A. Remmal, and A. Aboussekhra, “Eugenol potentiates cisplatin anticancer activity through inhibition of ALDH-positive breast Oxidative Medicine and Cellular Longevity cancer stem cells and the NF-κB signaling pathway,” Molecular Carcinogenesis, 2018, 57 (3): 333–346.
77. Priyadarshini, L.; Aggarwal, A. Astaxanthin inhibits cytokines production and inflammatory gene expression by suppressing IkappaB kinase-dependent nuclear factor kappaB activation in pre and postpartum Murrah buffaloes during different seasons. Vet. World 2018, 11, 782–788.
78. R. Nakao, O. L. Nelson, J. S. Park, B. D. Mathison, P. A. Thompson, and B. P. Chew, “Effect of dietary astaxanthin at different stages of mammary tumor initiation in BALB/c mice,” Anticancer Research, vol. 30, no. 6, pp. 2171–2175, 2010.
79. J.-P. Yuan, J. Peng, K. Yin, and J.-H. Wang, “Potential health-promoting effects of astaxanthin: a high-value carotenoid mostly from microalgae,” Molecular Nutrition & Food Research, 2011, 55 (1): 150–165.

80. P. Kidd, “Astaxanthin, cell membrane nutrient with diverse clinical benefits and anti-aging potential,” Alternative Medicine Review, 2011, 16 (4): 355–364.

Figures

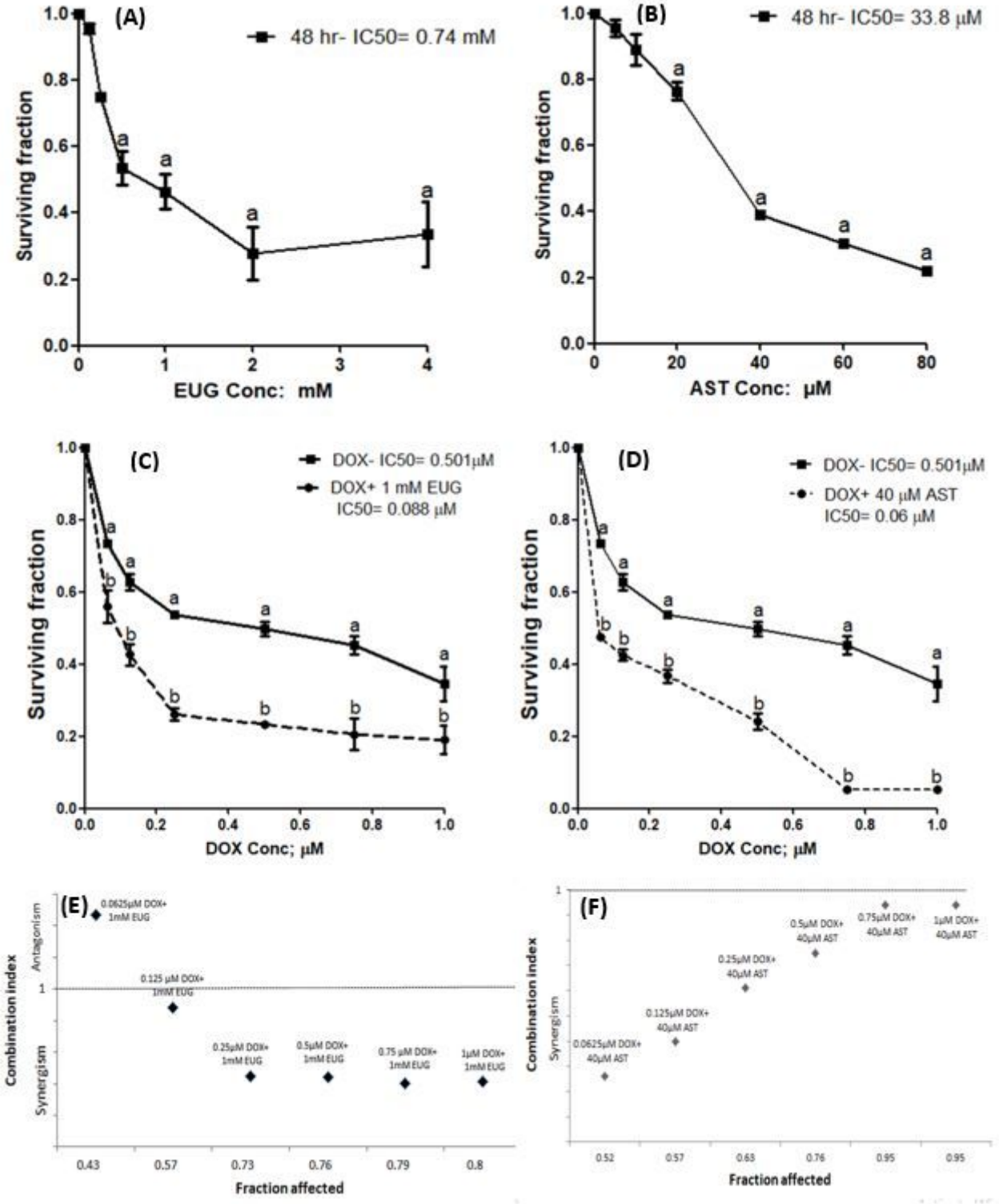

Figure 1

Effect of EUG (A), AST (B), DOX plus EUG (C) and DOX plus AST (D) on survival of MCF7 cells. The combination index produced from 1mM EUG (E) and 40μM AST (F) combinations with 0.25 μM DOX. Data are expressed as mean ± SD of three separate experiments, each performed in triplicates. a indicates significant change from control at P≤ 0.05 using one-way ANOVA followed by Dunette as a post ANOVA test and b indicates significant from DOX alone at P≤ 0.05 using student t-test.

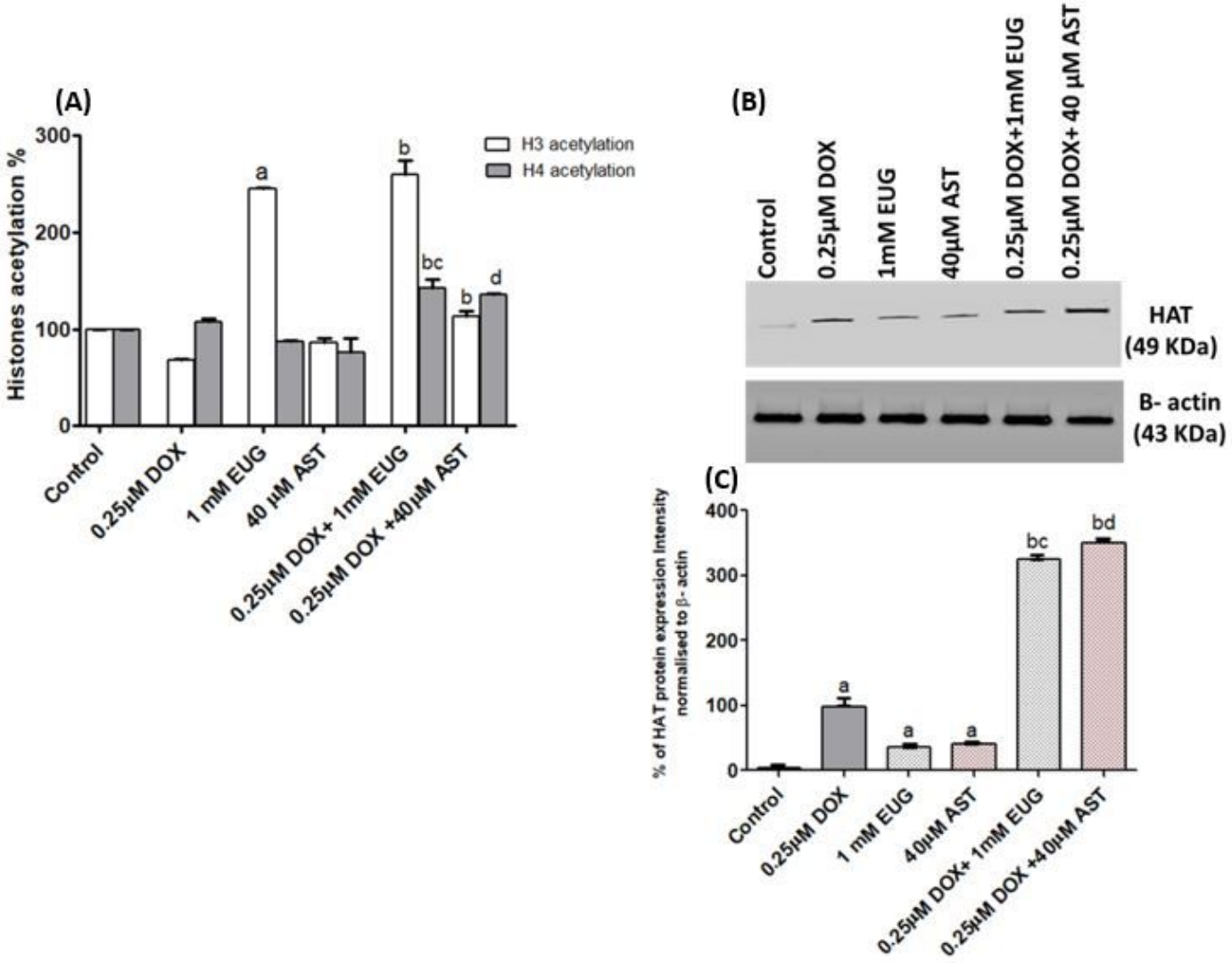

Figure 2

Effect of DOX, EUG, AST and their combination on Histones (H3 and H4) acetylation % (A), HAT protein expression (B), and % of HAT protein intensity normalised to β-actin (C). Data are expressed as mean ± SD of three separate experiments, each performed in triplicates. a,b,c and d indicate significant from control, DOX, EUG and AST, respectively at P≤ 0.05 using one-way ANOVA followed by Tukey-Kramer as a post ANOVA test.

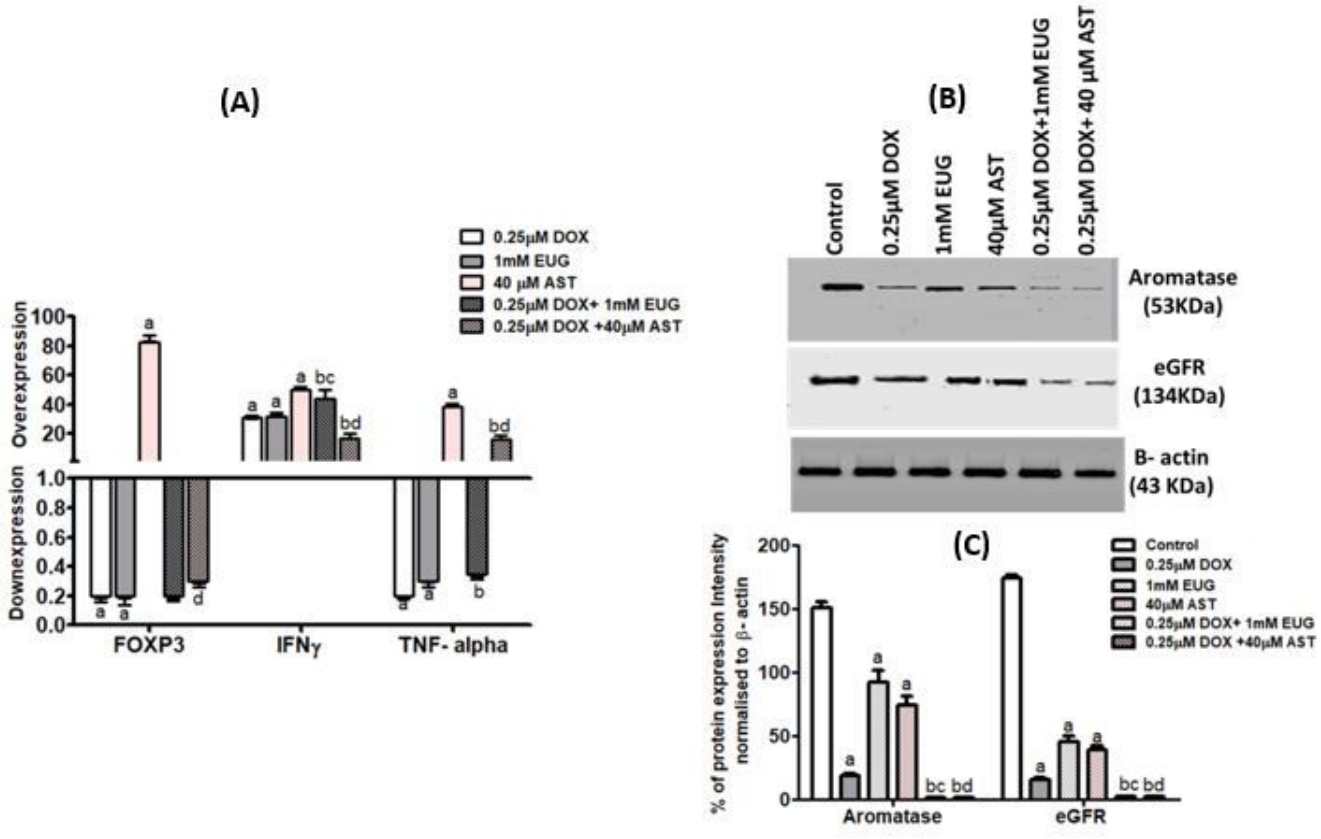

Figure 3

Effect of DOX, EUG, AST and their combination on FOXP3, IFNγ and TNFα mRNA expression (A), aromatase and eGFR protein expression (B), and % of aromatase and eGFR protein intensity normalised to β- actin (C). Data are expressed as mean ± SD of three separate experiments, each performed in triplicates. a,b,c and d indicate significant from control, DOX, EUG and AST, respectively at P≤ 0.05 using one-way ANOVA followed by Tukey-Kramer as a post ANOVA test.

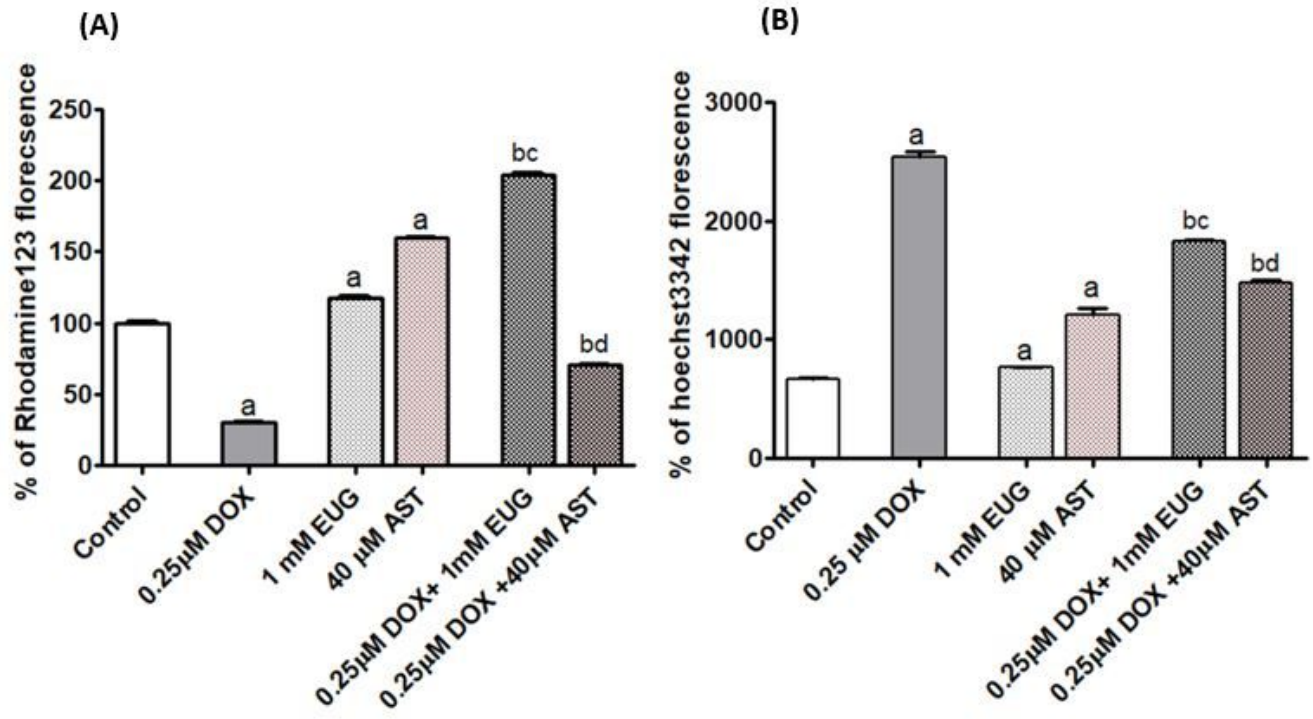

Figure 4

Effect of DOX, EUG, AST and their combination on % of rhodamine123 uptake (A) and % of hoechst3342 uptake (B). Data are expressed as mean ± SD of three separate experiments, each performed in triplicates. a,b, c and d indicate significant from control, DOX, EUG and AST, respectively at P≤ 0.05 using one-way ANOVA followed by Tukey-Kramer as a post ANOVA test.

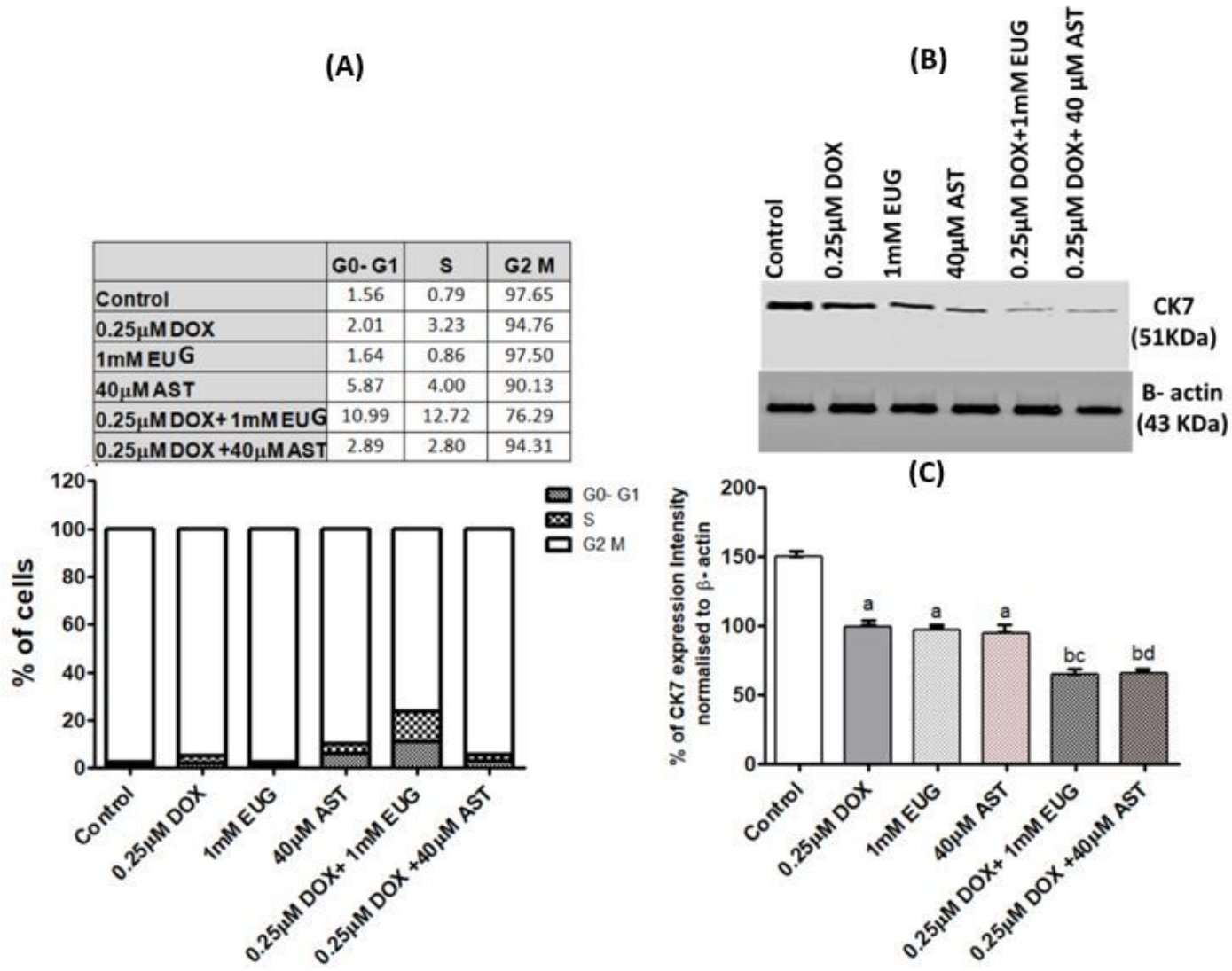

	G0- G1	S	G2 M
Control	1.56	0.79	97.65
0.25µM DOX	2.01	3.23	94.76
1mM EUG	1.64	0.86	97.50
40µM AST	5.87	4.00	90.13
0.25µM DOX+ 1mM EUG	10.99	12.72	76.29
0.25µM DOX +40µM AST	2.89	2.80	94.31

Figure 5

Effect of DOX, EUG, AST and their combination on % of cells at the phases of cell cycle (A), CK7 protein expression (B), and % of CK7 protein intensity normalised to β-actin (C). Data are expressed as mean ± SD of three separate experiments, each performed in triplicates. a,b, c and d indicate significant from control, DOX, EUG and AST, respectively at P≤ 0.05 using one-way ANOVA followed by Tukey-Kramer as a post ANOVA test.

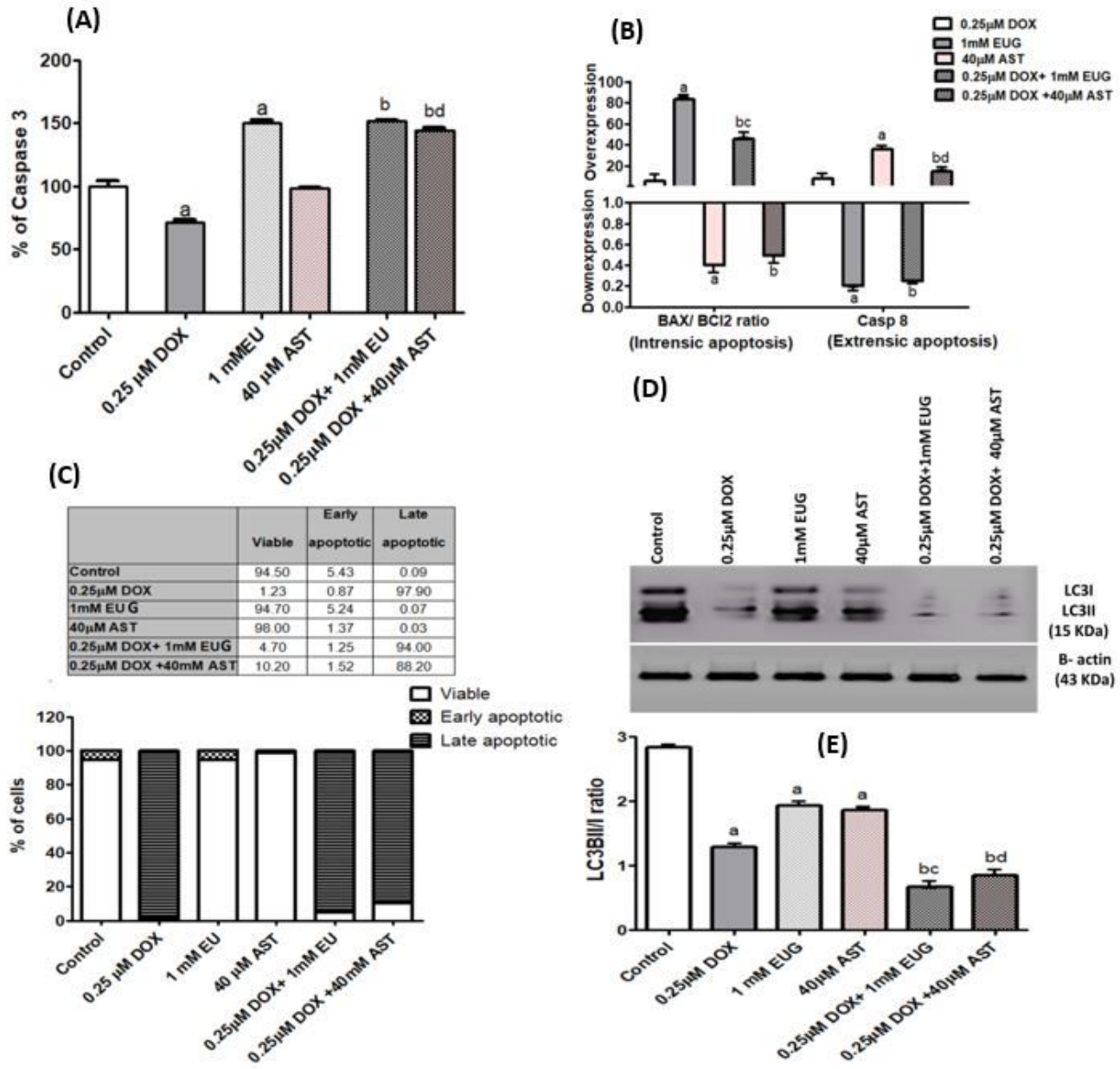

	Viable	Early apoptotic	Late apoptotic
Control	94.50	5.43	0.09
0.25µM DOX	1.23	0.87	97.90
1mM EUG	94.70	5.24	0.07
40µM AST	98.00	1.37	0.03
0.25µM DOX+ 1mM EUG	4.70	1.25	94.00
0.25µM DOX +40mM AST	10.20	1.52	88.20

Figure 6

Effect of DOX, EUG, AST and their combination on % of caspase 3 (A), mRNA expression of BAX, BCl2 and caspase 8 (B), % of cells according to propidium iodide staining (C), LC3I and LC3II protein expression (D), and LC3B II/I ratio (E). Data are expressed as mean ± SD of three separate experiments, each performed in triplicates. a,b, c and d indicate significant from control, DOX, EUG and AST, respectively at P≤ 0.05 using one-way ANOVA followed by Tukey-Kramer as a post ANOVA test.

Supplementary Files

This is a list of supplementary files associated with this preprint. Click to download.

- Suplementaryfileoriginalblots.docx